A LES Study of Wind-Shear Effect on Turbulent Structure of Stratocumulus Clouds

Shouping Wang[1], Christophe Jean-Golaz[2] and Qing Wang[3]

[1] *Naval Research Laboratory, Monterey, California*
[2] UCAR VSP, NOAA GFDL, Princeton, New Jersey
[3]*Naval Postgraduate School, Monterey, California*

1. INTRODUCTION

Turbulence dynamics of stratocumulus clouds has been investigated intensively for the past several decades. Most of the studies have been focused on the physical processes driven by or closely coupled to the cloud-top longwave radiative cooling. Most of the dynamical theories and parameterization schemes have been based on the implicit assumption that the wind shear across the inversion only plays a negligible role. However, some observations have shown that this wind shear can be very significant. Especially, in the west coast of central California, forced by the coast line and topography, the wind shear at the top of the stratocumulus-topped boundary layer can reach as high as 10 m/s across an inversion of only 50-100 m thickness (Kalogiros and Wang, 2002). In addition, recent observation and modeling show that the wind shear may play important role in regulating turbulent and mean structure in both clear and cloudy boundary layers (e.g., Moeng et al., 2005; Conzemius and Fedorovich, 2006)

In this work, we used a large-eddy simulation model to simulate an observed cloud-topped boundary layer and examine how the turbulence and mean structure respond to different wind shear profiles.

2. OBSERVATIONS

DECS (Development and Evolution of Coastal Stratocumulus) is a field experiment conducted in June, 1999 in the area off the coast of Monterey, California, aiming at understanding the physical processes in the clouds that are strongly driven by or linked to the mesoscale phenomena in the central California Coast, such as coastal topographical flow and the diurnal evolution of stratocumulus clouds (Kalogiros and Wang). During the experiment, strong wind shear across the inversion was frequently observed in aircraft measurements. Fig. 1 shows soundings made in aircraft flight on July 8, 1999. Owing to the dynamic influences of the coastal topography, the wind speed reaches maximum 18 m s^{-1} at the top of the boundary layer, and then decreases to 7 m s^{-1} at 250 m above the cloud top.

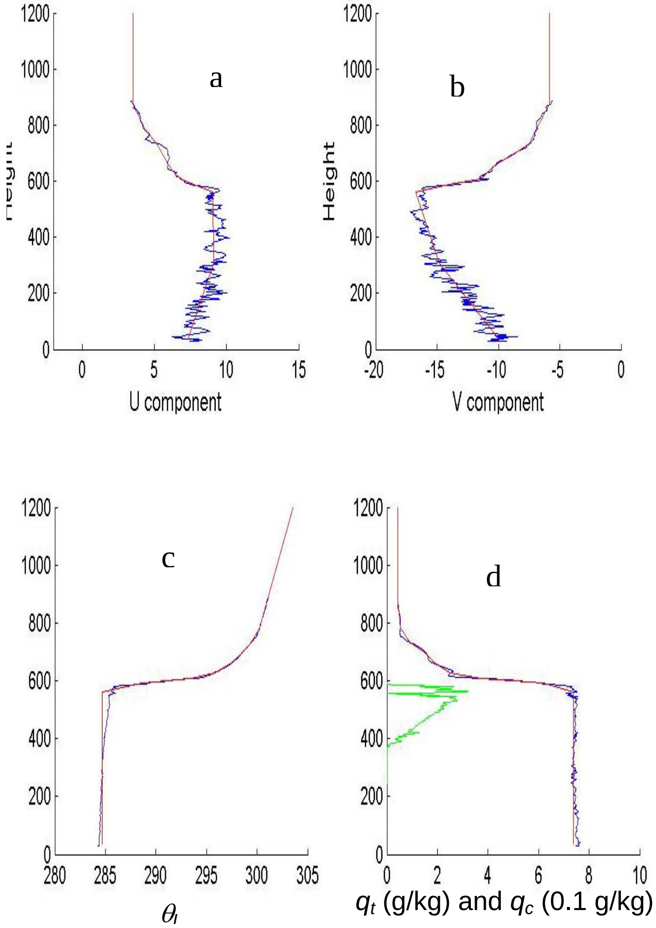

Figure 1: Aircraft soundings. a: west-east component of wind; b: the south-north component. c: liquid water potential temperature d: total water mixing ratio and liquid water mixing ratio. The read lines are averages of the respective soundings.

Corresponding author Address: Shouping Wang, NRL, Monterey, California 93943. wang@nrlmry.navy.mil

The temperature and moisture profiles indicate a well-mix boundary layer with sharp gradients at 600 m, above which they change more gradually. It is not clear, however, how thick the turbulent entrainment zone was and how much portion of the wind speed change actually occurred within the mixing zone in the inversion.

3. COAMPS-LES SETUP

Naval Research Laboratory's Coupled Ocean/Atmosphere Mesoscale Prediction System (COAMPS) is Navy's operational weather forecast model and was recently extended to perform as a LES model. COAMPS-LES has been successfully used to simulate various boundary layer regimes as discussed in Golaz *et al.* (2005). For this study, the model is configured to cover the domain of 5.4 km × 5.4 km × 1.3 km with the grid points distribution of 181 × 181 × 85. The horizontal grid spacing is 30 m; the vertical is varied between 20 to 5 m with the highest resolution in the inversion layer.

Sensitivity simulations are performed with two different wind shear profiles shown in Fig. 2, which are derived from those in Fig. 1. Because the wind profiles in Fig. 1 were largely driven by the mesoscale pressure gradient and the wind advection associated with the coastal topography, a proper mesoscale forcing needs to be applied to the COAMPS-LES to maintain the wind profile throughout the simulations. For this purpose, we separately run mesoscale COAMPS model for July 5-6, 1999, and evaluate the wind field and analyze the mesoscale forcing (not shown here). The mesoscale COAMPS run indeed qualitatively simulate the wind maximum in the boundary layer at the right time and locations, although the magnitude of the maximum is less and the inversion layer thickness is significantly larger than the observations. Since our interest is on the impact of wind shear on the turbulence, we simply derive a mesoscale forcing based on the COAMPS analysis, and then tune it to achieve the desirable wind profiles. Another issue is related to the turbulence spin-up with the strong wind shear. If the LES were initialized with the strong-shear wind profile, the spin-up would produce strong turbulence at the cloud top, which would rapidly destroy the cloud layer since the equilibrium structure is not yet established. Therefore, we start with a constant wind profile equal to the geostrophic wind above the inversion, and use a strong nudging term to force the wind to reach to those shown in Fig. 2 in the first hour, following which the nudging term is set zero. The observed temperature and moisture profiles in Fig 1 are directly used in the initialization.

COAMPS-LES is run for 8 hours to reach quasi-equilibrium state, and all the results presented here are either the averages or instantaneous fields between 7 to 8 hours.

4. RESULTS

Two simulations, a strong shear case (SS) and a weak shear case (WS), are performed with two different wind profiles shown in Fig. 2. Although the wind profiles (Fig. 2) from two cases are quite different within and above the inversion, their magnitudes in the well-mixed layer are very similar. Therefore, the difference in the structure can be attributed to the different wind profiles shown in Fig. 2. Both Fig. 1 and 2 show that the inversion layer from case SS is thicker than that from case WS. It is also noticed that the cloud water is reduced and the level of its maximum value is therefore lowered in SS compared with those in WS. The thermodynamic structure from case SS, particularly the liquid water, is closer to the observation shown in Fig. 1. Case SS results in a larger negative buoyancy flux near the cloud top and a smaller positive buoyancy flux in the cloud layer than WS (Fig. 4), suggesting that a stronger entrainment mixing in the inversion and a weaker radiative forcing within clouds in SS simulation.

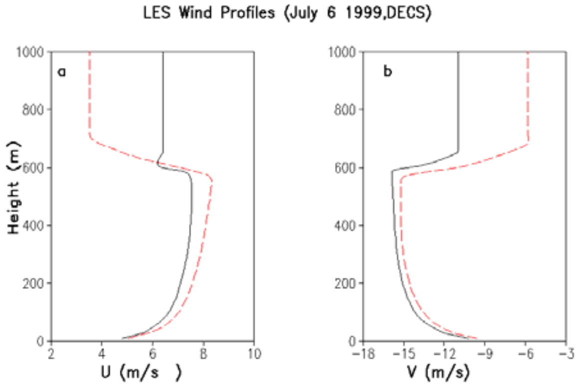

Figure 2. COAMPS-LES wind soundings from two simulations

Although both simulations produce similar $\overline{w'^2}$, they produce very different horizontal component of TKE in the inversion due to the strong shear, which also significantly increases the inversion layer thickness (Fig. 4). It is again noticed that the profiles from both simulations are very similar within the mixed layer with the slightly reduced values from SS.

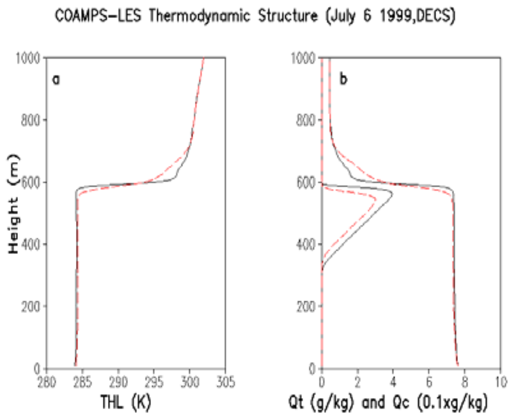

Figure 3. LES temperature and moisture soundings from two simulations. Red dashed lines are the results from "strong-shear" (SS) case. Black solid

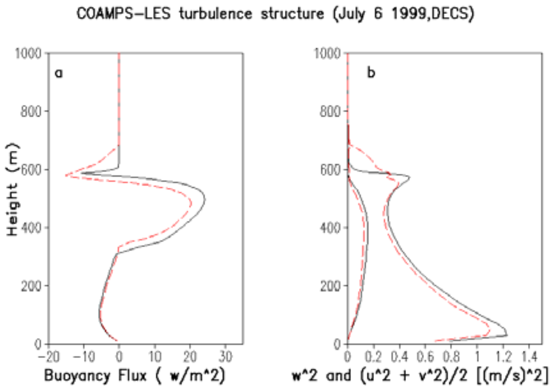

Figure 4. LES buoyancy flux, $\overline{w'^2}$ and $(\overline{u'^2}+\overline{v'^2})/2$ from two simulations. Red dashed lines are the results from "strong-shear" (SS) case. Black solid lines are those from "weak-shear" (WS) case.

Comparison of the TKE budgets in Fig. 5 shows major difference in the forcing in the inversion layer. For case WS, the balance in the budget is consistent with the typical radiatively driven energetics in the cloud layer and the inversion (Fig. 5a). For SS, the large shear production term in the inversion balances the negative contributions from the buoyancy, dissipation and transport. The wind-shear production in the inversion strengthens the turbulence intensity and thus increases the inversion thickness. Two TKE sources clearly operate in the different layers with the buoyancy flux in the cloud and the wind-shear in the inversion.

The shear instability in the inversion layer is responsible for the turbulence intensification, which is supported by the probability density distribution (PDF) of gradient Richardson number (R_i) calculated at two levels just above the inversion base from each simulation shown in Fig. 6. For case SS, the values are centered on 0.25 at both levels; for WS, the distribution is broader and shifts to larger values, reflecting the weak shear condition. A large percentage of grid points in case SS have the values of R_i that are less than the critical value 0.25, suggesting relatively intense shear-driven turbulence at both levels. In case WS, most of the grid points at 591 m have the R_i that are larger than 0.25, indicating weak turbulence intensity. The PDF of WS shifts to higher values with the mean of 0.8 at 601 m, which is consistent with the low TKE value (0.07) shown in Fig. 4.

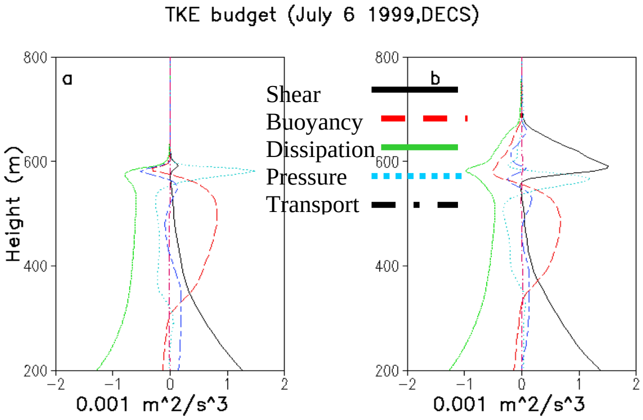

Figure 5. TKE budget from two simulations. a: Case WS; b: Case SS

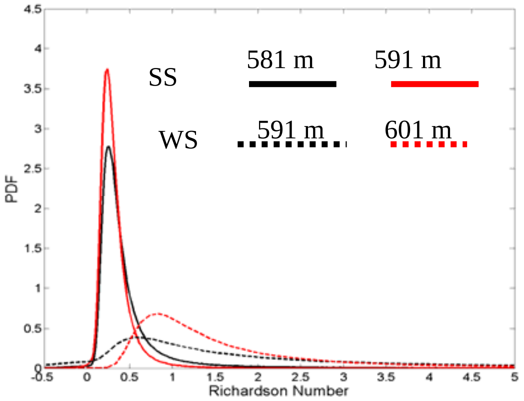

Figure 6: Richardson number distribution just above the inversion base for both SS and WS simulations.

Fig. 7 compares the instantaneous inversion structures derived from the LES simulations at 7.4 hours. The strong shear introduces significant variability in flows, which includes both wave and turbulent motions. The horizontal wind components particularly show large variations in both y and z directions at and above the local cloud-clear air interface

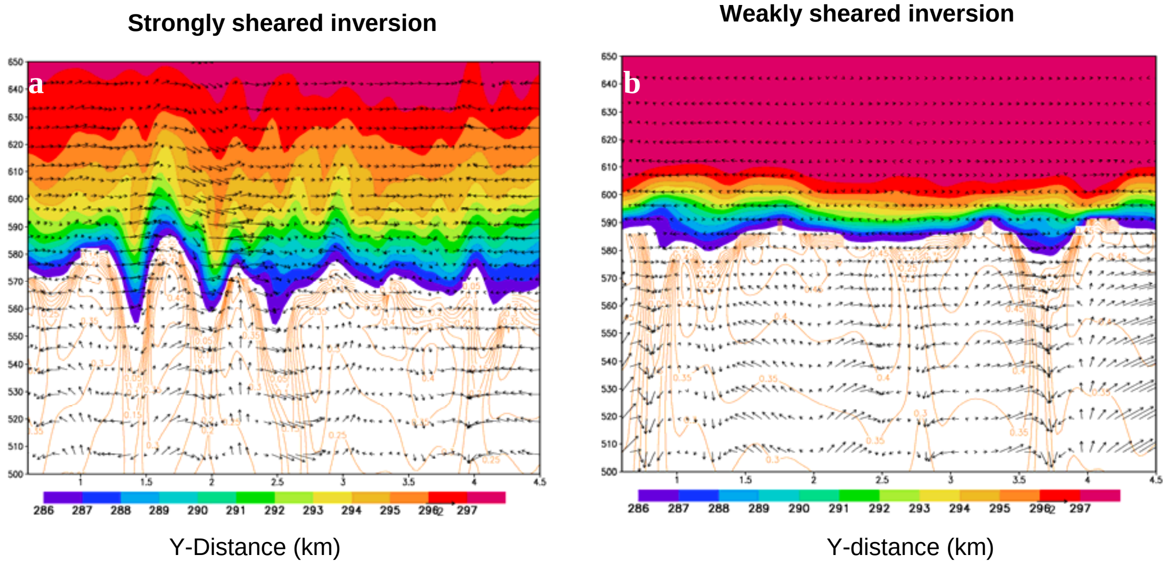

Figure 7. Examples of interface structure from the LES simulations at x=3km. Colored shading: Potential temperature; Contours: Cloud water content; Vectors: Turbulent fluctuate motion. Left: SS simulation; Right: SS simulation.

The intensified local mixing due to the strong shear reduces the liquid water and thus lowers the cloud-top height in simulation SS. There appear to be several entrainment events at y ∈ (1.4 km, 2 km, 2.5 km), where wisps of warm and dry air are pulled into the cloudy mixed layer (Fig. 7a). These events can be compared with those similar in case WS as shown at y ∈ (0.5 km, 3.75 km) in Fig. 7b. One major difference is that the downdrafts associated with the entrainment events from SS are weaker and have broader areas than those from WS.

5. SUMMARY

Wind shear across the inversion has long been recognized to intensify the entrainment mixing at the boundary layer top, which should supposedly lead to a higher cloud-top height. Our simulation shows that despite the strong entrainment mixing due to the wind shear, the cloud-top height slightly decreases in case SS. The main reason for this decrease is that the shear-driven mixing primarily occurs within the inversion layer and the liquid water is reduced as the result of the mixing, which leads to the reduction of the radiative cooling and decrease in TKE in the cloud layer. Consequently, the cloud-top height is lowered and the inversion layer thickens.

The presence of clouds clearly complicates the process in which the wind shear affects the entrainment. On one hand, the shear enhances the turbulence intensity and increases the entrainment mixing; on the other hand, the mixing decreases the cloud water and the radiative cooling, which tends to an overall reduction in turbulence intensity in the cloud layer. Furthermore, because the shear-driven mixing mainly occurs within inversion, its thickness increases significantly. Consequently, one has to ask to what extent the mixed-layer jump model still applies under the strong wind-shear condition.

REFERENCE

Conzemius, R. J., and E. Forodovich, 2005: Dynamics of sheared convective boundary layer entrainment. Part I: Methodological background and large-eddy simulations. *J. Atmos. Sci.,* In press

Golaz, J.-C., S. Wang., J. D. Doyle and J. M. Schmidt, 2004: COAMPS^{TM} LES: Model evaluation and analysis of second and third moment vertical velocity budgets. *Bound. Layer Meteo. 116,* 487-517.

Kalogiros and Wang, 2001: The California low-level coastal jet and near shore stratocumulus. Coastal Meteorology

Moeng, C.-H., B. Stevens, and P. P. Sullivan, 2005: Where is the interface of stratocumulus-topped PBL? *J. Atmos. Sci.*, 62, 2626-2631.